PHYSICAL REVIEW C VOLUME 31, NUMBER 1 JANUARY 1985

Fragmentation instabilities in nuclear systems

A. D. Panagiotou
National Superconducting Cyclotron Laboratory, Michigan State University, East Lansing, Michigan 48824 and Department of Physics, Nuclear Physics Laboratory, University of Athens, Athens, Greece

M. W. Curtin and D. K. Scott
National Superconducting Cyclotron Laboratory, Michigan State University, East Lansing, Michigan 48824
(Received 31 July 1984)

The fragmentation of nuclear systems, formed in proton- and heavy-ion-induced reactions in a wide energy range, is examined. The dependence of the fragment production cross section on the incident energy and on the temperature of the emitting source is compared to predictions of a theory of condensation. We find many instances where the fragmentation instability can be explained by and may be attributed to a liquid-gas phase transition. Our analysis suggests the occurrence of instabilities at a critical temperature of approximately 11 to 12 MeV, in accord with several theoretical predictions. Conventional nuclear effects, such as Coulomb barrier penetration, cannot fully describe the observed phenomena.

I. INTRODUCTION

The emission of intermediate-mass fragments from nuclear systems, created in proton- and heavy-ion-induced reactions at intermediate and high energies, has attracted much attention recently. At these energies novel phenomena of the transient highly excited nuclear system may occur, manifesting themselves through multifragmentation and pion production processes. Through the use of high energy nuclear collisions it may become possible to create new forms of nuclear matter and to determine the nuclear equation of state.[1] Although most attention has been directed towards such phenomena as phase transitions to a pion condensate or a quark-gluon plasma, conjectured to develop at high density and temperature, it is also possible that a liquid-gas phase instability may set in at a much lower critical temperature and density.[2,3] This instability may be encountered during the expansion of the initially heated zone, formed in an energetic nuclear collision, and manifest itself through the emission of complex nuclear fragments.

Studies of the formation of complex fragments in proton- and heavy-ion-induced reactions in a wide energy range are of intrinsic interest in yielding information on the equation of state at moderate temperatures and at densities below normal. They also provide insight into the hydrodynamical behavior, necessary for the occurrence of more exotic phase transitions and for the astrophysical ramifications with regard to neutron stars and supernovae.[4,35]

The fundamental question of how a highly excited, low density nuclear system disassembles is the aim of much theoretical and experimental work (Refs. 2–9 and references therein). There are several difficulties, however, in realizing this goal: Since nuclear reactions are time dependent phenomena, it is not readily apparent whether there is sufficient time—at the energies under consideration—for a state of thermal and chemical equilibrium to evolve. Furthermore, are we justified to talk about thermal and chemical equilibrium in a system of a small number of particles, of the order of ~ 100? Would a phase transition—if it exists—be washed out due to finite particle number effects? There is also the question of the expansion and cooling of the heated system and the fragmentation process throughout this stage. What are the differences, if any, in the fragmentation process of the initially heated zone between proton- and heavy-ion-induced reactions? Which type of reaction may be a better probe of nuclear instabilities and may give an unambiguous signature of possible phase transitions?

In this paper we analyze and present possible experimental evidence for fragmentation instabilities which support the notion of a liquid-gas (LG) phase transition in the expanding hot nuclear system. In Sec. II, we present the relevant theory for LG phase change. In Sec. III, we analyze fragment distributions from several proton- and heavy-ion-induced reactions on medium and heavy targets in the energy range between 0.18 and 350 GeV. Finally, we show that "conventional" phenomena, such as Coulomb barrier effects, cannot fully account for the observed behavior of the fragment distributions. Appropriate experiments for a systematic study of the LG phase transitions are proposed.

II. LIQUID-GAS PHASE TRANSITION

A. Equation of state

The properties of nuclear matter at finite temperatures and densities below normal ($\rho_0 = 0.17$ fm^{-3}) have been studied extensively.[10–12,36] It has been shown that in the Hartree-Fock approximation the nuclear matter exhibits the same properties as a van der Waals system.[11] Calculations of the equation of state, assuming a uniform density and phenomenological or realistic interactions,[5,12] have produced isothermal, pressure versus density curves simi-

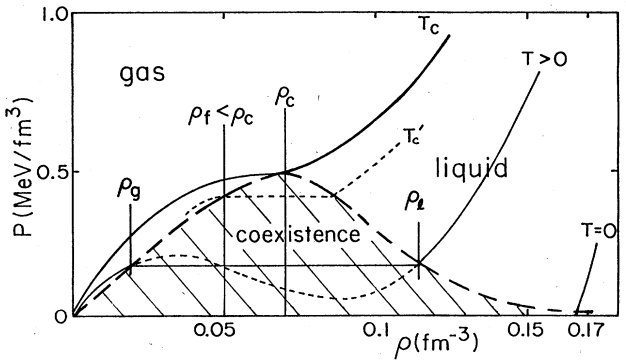

FIG. 1. Pressure versus density for nuclear matter. The three regions, liquid, LG coexistence, and gas, are indicated (also see the discussion in the text).

lar to those in Fig. 1. The magnitude of the critical quantities, ρ_c and T_c, for a liquid-gas phase transition vary in the range 0.2—0.4 ρ_0 and 8—20 MeV, respectively, depending on assumptions and initial conditions.

During the expansion and disassembly phase of the hot region along an isotherm (isentropic expansion with changing temperature and constant entropy has also been discussed by other authors[8,9]), the nuclear density decreases until the freeze-out density, ρ_f, is reached. This density is defined as the density at which the mean free path of the emitted fragments is commensurate with the size of the hot region. At ρ_f, collisions cease and the fragments move undisturbed, aside from final state interactions and internal deexcitation.[13] To observe both liquid and gas phases at a certain temperature, the Maxwellian construction must encompass ρ_f. This construction is equivalent to equating the pressures and the chemical potentials of the two phases.

If ρ_f is large, the system will be mostly in the liquid phase at freeze out, whereas if ρ_f is very small, the system will have traversed the coexistence region and only the gas phase will exist. In the case that $\rho_f < \rho_c$, the system will enter the gas phase prior to freeze out, causing an erroneous interpretation of T' as the critical temperature T_c. If, however, $\rho_f > \rho_c$, the temperature T_c will be correctly identified. The quoted value of ρ_f is $0.4\rho_0$,[14] which is approximately equal to or somewhat larger than the range of calculated ρ_c values. As shown in Fig. 1, we can expect the following evolution of the system: As the density decreases during expansion along an isotherm and the system enters the metastable region of LG coexistence, the nuclear matter breaks into two pieces, one in the liquid phase with density ρ_f and the other in the gas phase with density ρ_g. It is the nuclear matter in the gas phase which condenses upon cooling to the complex fragments. As the temperature increases, the two densities approach each other, finally coinciding at the critical density, ρ_c, defined by the condition

$$dp/d\rho = d^2F/d\rho^2 = 0 ,$$

at constant temperature. For higher temperature only one phase exists, that of a gas.

The possibility of a phase transition in a thermally equilibrated nuclear system was previously considered theoretically in a number of papers.[4–6,15] It has been suggested[16] that the power law dependence of the fragment distributions, emitted by an equilibrated nuclear system, may constitute a signature for the occurrence of phase transition phenomena near a critical point. The widely differing systems,[7,17–22] which exhibit this characteristic approximate power law dependence, suggest that phase transitions are global in nature, dependent only on the energy imparted to the fragmenting system.

B. Theory of condensation

Following the treatment of Refs. 4, 23, and 2 in the framework of a theory of condensation in excited nuclear matter, the probability for fragment formation of size A is given by

$$P(A) \sim A^{-k} \exp\{[-a_{s'}(T)A^{2/3} - a_{v'}(T)A + \mu(T)A]/T\} , \tag{1}$$

where k is the T- and A-independent critical exponent, $a_{s'}(T) = a_s(T) - TS_s$ is the surface free energy per particle, $a_{v'}(T) = a_v(T) - TS_v$ is the volume free energy per particle, and $\mu(T)$ is the chemical potential per particle. The preceding relation can be written in the following form:

$$P(A) \sim A^{-k} X^{(A^{2/3})} Y^A , \tag{2}$$

where

$$X = \exp[-a_{s'}(T)/T] , \tag{3}$$

$$Y = \exp\{-[a_{v'}(T) - \mu(T)]/T\} . \tag{4}$$

With this substitution, Eq. (1) assumes the following three forms, corresponding to the three regions of Fig. 1 (see Ref. 2):

$$P(A) \sim A^{-k} X^{A^{2/3}}, \text{ for } T < T_c , \tag{5}$$

$$P(A) - A^{-k}, \text{ for } T = T_c , \tag{6}$$

$$P(A) - A^{-k} Y^A, \text{ for } T > T_c . \tag{7}$$

We note that X and Y are less than 1.0 for all $T \neq T_c$ and that the pure power law dependence of the fragment distributions at $T = T_c$ [Eq. (6)] is modulated by the exponential factors X and Y at temperatures $T < T_c$ and $T > T_c$, respectively.

Figure 2 shows indicatively the expected dependence of the fragment distributions on the temperature of the emitting system for three temperatures: $T < T_c$, $T = T_c$, and $T > T_c$. The curves were calculated using the parametrization of Ref. 2 for Eqs. (5) and (7) in the preceding and assuming $k = 2.0$ and $T_c = 12.0$ MeV. The slope of the distributions for both $T < T_c$ and $T > T_c$ is steeper than the slope for $T = T_c$ and should approach it as the temperature approaches T_c from below or above, respectively. As a consequence, the ratio of the cross section, $R = \sigma(A_1)/\sigma(A_2)$, of any two masses of the distribution, where $A_1 < A_2$, should increase as the temperature moves away from T_c, since $\sigma(A_2)$ decreases faster than $\sigma(A_1)$

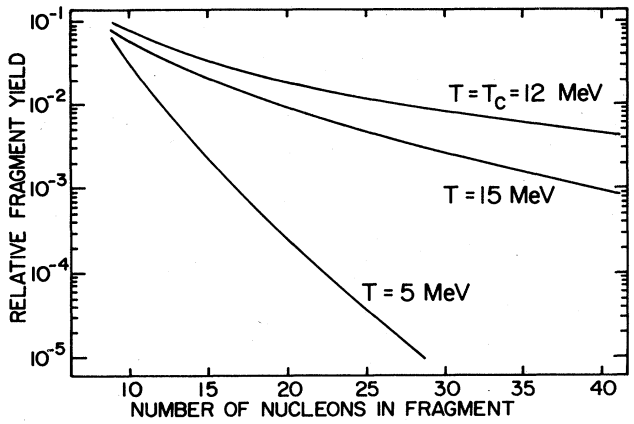

FIG. 2. Fragment distributions plotted on a relative scale for three temperatures of the emitting system. A critical exponent $k=2.0$ and a critical temperature $T_c=12.0$ MeV were assumed.

with temperature. This effect is more pronounced the larger the difference between the two masses.

III. ANALYSIS OF FRAGMENT DISTRIBUTIONS

A. Cross section ratios

The change of the slope of the fragment distributions with temperatures (Fig. 2) should manifest itself also as a function of incident energy, since the temperature of the emitting system is directly related to the imparted energy. Therefore, the ratio of the cross section for two different masses should also vary with incident energy in a predictable manner. Figure 3 shows the dependence of the ratio of the fragment cross section for $Z=6$ to that for $Z=12$ on the incident energy, for the systems C + Au and Ne + Au in the energy range of 15—84 and 250—2100 MeV/nucleon, respectively.[7,17,22] The ratio for C + Au is normalized to 1.0 at the 15 MeV/nucleon point and for Ne + Au at the 250 MeV/nucleon point.[37]

We observe that this ratio, which directly reflects the slope of the fragment distributions, decreases as the incident energy increases up to about 50 to 60 MeV/nucleon, and then the trend appears to be reversed at higher energies. A likely interpretation of this behavior is that for C + Au, the fragment emitting hot system reaches the critical temperature at some incident energy between 30 and 84 MeV/nucleon, corresponding to the minimum value of the ratio. The indication from the Ne + Au system is that, as the temperature further increases with increasing incident energy, the ratio increases as well.

Proton-induced fragmentation exhibits a somewhat different behavior in that limiting energy deposition in the target by the proton beam sets in at high energies. This is reflected in the limiting cross section for fragment production, shown in Fig. 4. Correspondingly, we should also expect a limiting temperature in the fragment-emitting system. This is shown in Fig. 5, where the temperature, calculated by moving source fits to the fragment distributions, is plotted as a function of the incident energy. Since the temperature of the system reaches a limiting value for energies higher than a few tens of GeV, the slope of the fragment distributions should also reach a limit at these energies.

This behavior is exhibited in Fig. 6, where we plot the ratio of the total cross section for the nuclides ^{18}F and ^{24}Na (shown in Fig. 4) produced in proton-induced reactions on Ag, Kr, and Xe in the incident energy range between 0.48 and 350 GeV.[19,24,25] We observe that this ratio—normalized to 1.0 at the 0.48 GeV point—reaches a minimum value at an incident energy of the order of 5 GeV and then increases to a limiting value at very high energies (see also Fig. 9). The apparent minimum in the

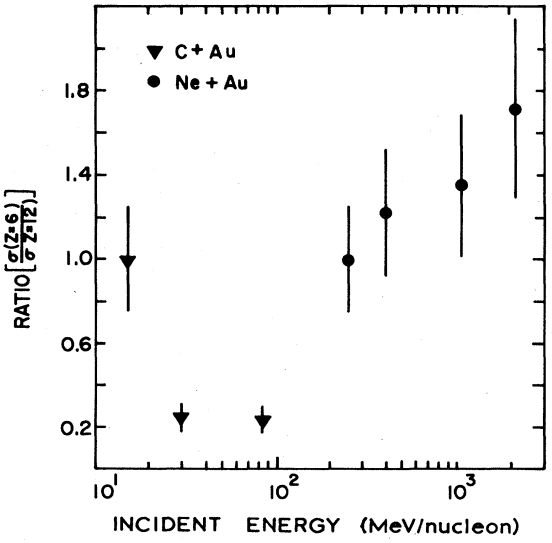

FIG. 3. The ratio of the cross section for $Z=6$ to 12 as a function of the incident energy per nucleon. The 15 and 250 MeV/nucleon points are normalized to 1.

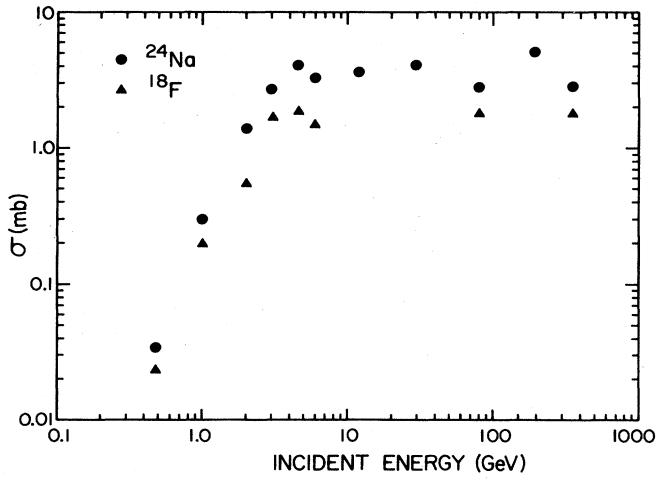

FIG. 4. Excitation functions of the yield of ^{18}F and ^{24}Na in proton-induced reactions on Ag and Kr,Xe (the points at 80 and 350 GeV). The errors are of the order of 10%.

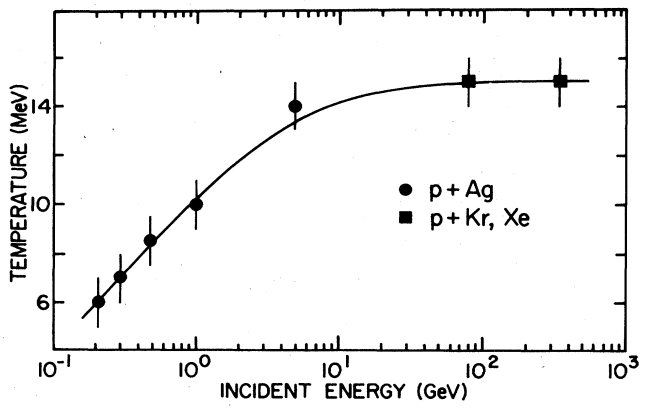

FIG. 5. The temperature of fragment-emitting systems versus the proton incident energy. The temperatures are obtained from moving source fits to the fragment energy distributions.

ratio at about 5 GeV may indicate that the system has reached the critical temperature near this incident energy. The difference between Figs. 3 and 6 is that in the former the ratio keeps increasing as the incident energy increases above a certain value, reflecting the continuous increase of the temperature of the system with energy.

B. Power law fits

To further elucidate the temperature dependence of the fragment production cross section, we fitted the available fragment distributions with a power law dependence of the form

$$P(A) \sim A^{-\tau}, \tag{8}$$

where τ is the "apparent" exponent. In this approximation, valid close to the critical point, the effects on the fragment emission of the temperature-dependent factors X and Y at $T < T_c$ and $T > T_c$, respectively [Eqs. (5) and (7)], are absorbed into the power exponent. Therefore, the apparent exponent *will vary with temperature* and will

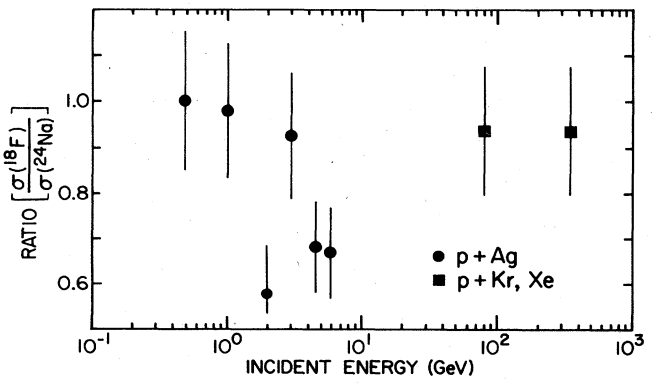

FIG. 6. The ratio of the total cross section of ^{18}F to ^{24}Na as a function of the incident proton energy. The 0.48 GeV point is normalized to 1.

reach a minimum value, that of the critical exponent k, at the critical temperature. This means that $\tau > k$ for all temperatures except $T = T_c$, where $\tau = k$.

Since the production cross section of light fragments ($Z < 3$) is affected by the sequential decay of heavier fragments, and for $Z = 4$ the most prolific isotope ^{8}Be is particle unstable, we fitted the fragment distributions only for $Z \geq 5$ or $A \geq 11$.[26] An additional reason for this choice of the minimum Z, A values is that the liquid-drop expansion, used to obtain Eq. (1), is valid only for large enough droplets.[4] Care was taken to avoid contributions from the tail of possible fission fragments. For some of the analyzed data the temperature of the system has been extracted from moving source fits to the fragment energy distributions, as reported in Refs. 19–21 and 27. Where the temperature was not given, we determined it either from the slope of the 90 energy distributions of the fragments,[18] or from ideal Fermi-gas calculations, assuming the size of the emitting system to be in the range of 2–4 times the largest fragment mass.[17,22] We assumed a ± 1.0 MeV uncertainty in establishing the source temperature. This assumption is quite realistic. In the case of the Fermi-gas calculations for the systems C + Ag and C + Au, it corresponds approximately to a source size of $A = 82 \pm 28$ and $A = 120 \pm 50$ nucleons, respectively.

Table I summarizes the data used and the values of the apparent exponent obtained by the fit. Figure 7 shows the quality of typical least-squares fits to the fragment mass distributions for several systems and energies. The approximate power law dependence is evident. In Fig. 8 we plot the apparent exponent, τ, as a function of the temperature of the emitting system. We observe a dramatic temperature dependence of the apparent exponent: τ decreases as the temperature increases up to about 11 to 12 MeV and then the trend is reversed. The exponent appears to reach a minimum value of approximately 2.0, a theoretically minimum value, in the temperature range of about 11–12 MeV. If we assign the critical temperature, T_c, to the temperature corresponding to the minimum value of the apparent exponent, τ, viz., corresponding to the maximum probability for fragment emission, then from Fig. 8 we may infer that $T_c \sim 11$–12 MeV.

Recently, an estimate of the critical temperature from fitting isotopic yields[16] gave a very low value of 3.3 MeV, although the temperature extracted from their fragment energy distributions was in the region of 15 MeV.[27] A possible explanation of this discrepancy is that, in fitting the isotope yields, the particle decay of the abundant excited neutron-rich (proton-rich) isotopes was not taken into account. Furthermore, not only the nuclei produced in excited states above the very low neutron (proton) emission threshold [$B_{n(p)} \geq 0.3$ MeV] will decay, but a large portion of those originally formed in the ground state will also decay, due to the continuous nucleon-fragment final state interaction (inelastic excitation) in the exit channel.[38] This interaction may result in a substantial "cooling" of the system.[39] Therefore, the measured isotope yield may by far not reflect the actual yield produced in the hot system, and consequently the system's temperature, as determined by the fit to this isotope distribution.

Calculations for finite nuclear systems,[28] using a

TABLE I. Summary of the data used and the values of the apparent exponent, obtained from the power law fit to the fragment distributions.

System	Energy (GeV)	Fragment range	Apparent exponent	Temperature (MeV)	Reference
p+Ag	0.21	$5 \leq Z \leq 8$	4.7±0.3	6.0	18
p+Ag	0.30	$5 \leq Z \leq 8$	4.4±0.3	6.7	18
p+Ag	0.48	$11 \leq A \leq 25$	3.5±0.2	8.2	19
p+Ag	4.90	$5 \leq Z \leq 18$	2.3±0.2[a]	14.0	20
p+Kr	80—350	$11 \leq A \leq 30$	3.0±0.2[b]	14.5	25
p+Xe	80—350	$11 \leq A \leq 30$	3.0±0.2[b]	15.0	25
p+U	4.90	$6 \leq Z \leq 11$	2.0±0.2	13.5	20
p+U	5.50	$5 \leq Z \leq 11$	2.0±0.2	12.6	21
C+Ag	0.18	$5 \leq Z \leq 22$	3.6±0.2	5.6	17
C+Ag	0.36	$5 \leq Z \leq 13$	2.7±0.2	7.7	17
C+Au	0.18	$5 \leq Z \leq 11$	4.9±0.2	4.9	17
C+Au	0.36	$5 \leq Z \leq 11$	3.2±0.2	7.2	17
C+Au	1.01	$6 \leq Z \leq 20$	2.5±0.3[c]	13.4	22

[a]The differential cross section at 90° is multiplied by 4π.
[b]Only differential cross sections at 34° (see Ref. 27).
[c]Only differential cross sections at 20°.

Skyrme effective interaction and finite temperature Hartree-Fock theory and assuming a ground state binding energy of 8 MeV/nucleon, predict the critical temperature to be in the range of 9.5—13.5 MeV, depending on the value of the effective mass and the power of the density dependence. Recent Hartree-Fock calculations at finite temperature,[10] which include the contribution of unbound states and use Skyrme SIII and SKM interactions, predict a critical temperature of 11 and 8 MeV, respectively. Furthermore, evaluation of thermal properties of finite nuclei,[29] using the thermal Hartree-Fock approximation and the Skyrme III interaction, yield a critical temperature $T_c = 11.8$ MeV for the liquid drop surface tension. Similarly, extended Fermi-gas model calculations,[30] in which the potential energy is treated within Bruekner's energy-density formalism and appropriate corrections due to surface and asymmetry effects were included, predict a diminishing surface tension at a critical temperature of approximately 11 to 13 MeV, for a nuclear compressibility constant K in the range of 180—250 MeV. Finally, a semiclassical treatment of hot semi-infinite nuclear matter,[36] using a realistic Skyrme force, predicts a vanishing surface-free energy at the critical temperature of 14.6 MeV and critical density of $0.33\rho_0$. All of the preceding theoretical predictions are in good agreement with the estimation of the critical temperature from our analysis.

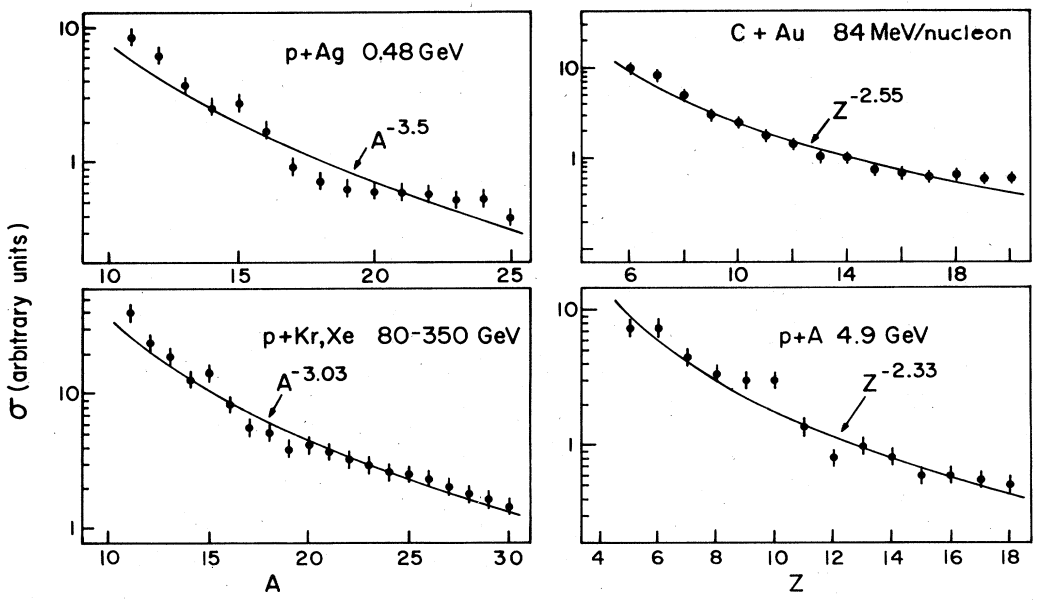

FIG. 7. Typical power law least-squares fits to the fragment mass distributions.

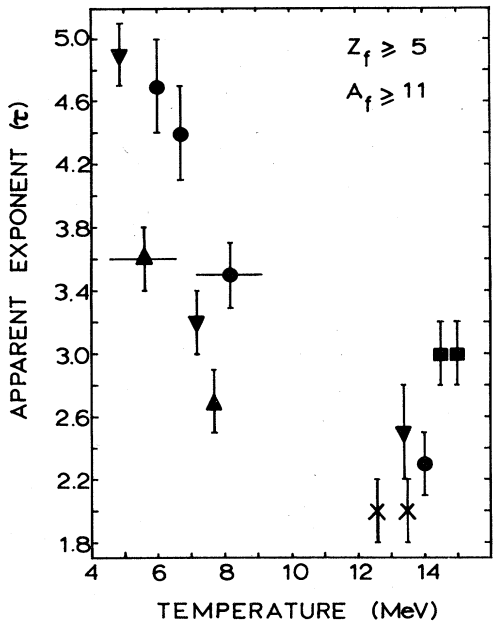

FIG. 8. The apparent exponent, τ, of the power law fit to the fragment distributions as a function of the temperature, T. The systems are as follows: circles—p + Ag; crosses—p + U; squares—p + Xe and p + Kr; triangles—C + Ag; and inverted triangles—C + Au.

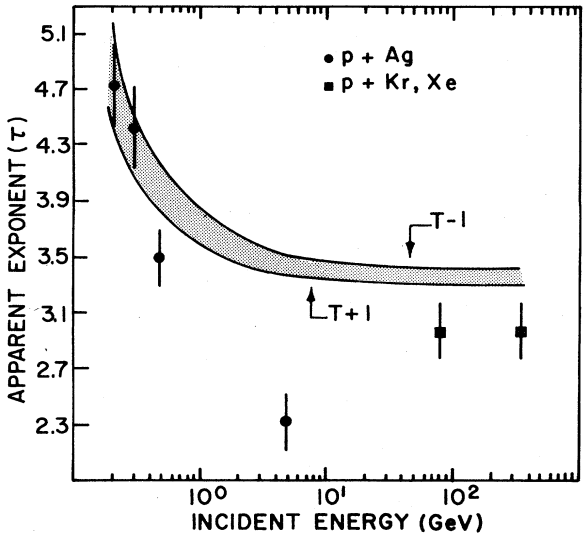

FIG. 9. The apparent exponent, τ, as a function of the incident energy for the systems p + Ag and p + Kr,Xe. The curves depict the dependence of the calculated apparent exponent on the Coulomb barrier effects (see the discussion in the text).

C. Excitation functions

The analysis in Sec. III B made use of fragment distributions from widely differing systems and with an uncertainty in the temperature of the source. To circumvent this inherent difficulty one should choose one system, measure an excitation function of the fragment distributions, and study the dependence of the apparent exponent on the incident energy.

In this framework we examined the excitation function of the complex fragment distributions emitted in p + Ag reactions in the energy range of 0.21–4.9 GeV,[18–20] and in p + Kr,Xe in the energy range of 80–350 GeV.[25] The latter reactions produced similar fragment distributions for both targets, an indication that in this energy range there is very little or no target-mass dependence for $84 \leq A(\text{target}) \leq 132$. This analysis is temperature independent and, therefore, it is free of the uncertainty due to the inherent difficulties in accurately establishing the temperature of the source emitting the fragments.

In Fig. 9 we plot the apparent exponent, τ, as a function of the incident proton energy (see Table I). We observe that the exponent decreases with increasing energy up to about 5–6 GeV and then the trend is reversed, leveling off at very high energies. In spite of the scarcity of data points in the energy range of between 0.3 and 80 GeV, there is an indication for a departure from a smooth and asymptotic behavior. It has been suggested that Coulomb barrier effects between the source and the emitted fragments may account for a smooth dependence of the fragment yield on the temperature.[31,32] The smooth dependence comes from the barrier penetrability factor, which is temperature dependent. That is, the higher the temperature contained in the source, the smaller the Coulomb barrier hindrance to the fragment emission and, therefore, the larger the fragment cross section.

IV. COULOMB CURVES

To obtain a quantitative picture of the smooth behavior of the Coulomb effects, we calculated the decrease of the fragment production cross section due to the Coulomb barrier penetration.[32] We assume that the fragment-emitting source has a size of $A,Z=70,30$ and temperatures of 6 ± 1, 7 ± 1, 8 ± 1, 14 ± 1, and 15 ± 1 MeV, corresponding approximately to incident energies of 0.21, 0.3, 0.48, 4.9, and 80–350 GeV, respectively (see Table I). The Coulomb barrier penetrability was calculated for each temperature by the expression

$$P(A) \sim \exp\left[-2\int^{R_f}\{2m/\hbar^2[V(x)-E]\}^{1/2}dx\right], \quad (9)$$

where R_f is $R(V=E)$, m is the nucleon mass, V is the Coulomb barrier seen by each fragment, and E is the distribution of the fragment kinetic energy before emission at each temperature. This treatment of the fragment emission is very similar to alpha-particle emission after penetration through the nuclear Coulomb barrier. The penetrability factor is multiplied by the fragment yield at the high energy region $[Y(A) \sim A^{-3.0}]$. The resulting mass distributions for $11 \leq A \leq 25$ were fitted by a power law of the form

$$A^{-\tau} \sim P(A)A^{-3.0}. \quad (10)$$

The Coulomb curves obtained from this calculation are shown in Fig. 9, only normalized to the 0.21 GeV point. The spread of the curves reflects the assumed ±1 MeV uncertainty in the temperature of the source at each ener-

gy. The smooth and asymptotic dependence of the apparent exponent, incurred when Coulomb effects are incorporated, is evident. The departure from this shape—a smooth curve joining the 0.48 and 80 GeV points, which is at least 2 standard deviations at the 4.9 GeV point—indicates that conventional phenomena do not fully account for the observed fragmentation systematics.

V. SUMMARY AND CONCLUSIONS

In this paper we presented experimental evidence that fragmentation instabilities in hot nuclear systems may be viewed as signatures for liquid-gas phase transitions. A theory of condensation was used to analyze and interpret the fragmentation systematics and it has been possible to account for most of the features of a wide range of data. The critical temperature of a phase transition, obtained from our analysis of the complex fragment distributions in proton- and heavy-ion-induced reactions, is within the range of several theoretical calculations. Although no systematic experimental study of critical phenomena has as yet been reported, the available data on fragment production from diverse systems may indicate the existence of phase instabilities with a critical temperature in the region of 11—12 MeV and a critical exponent of perhaps less than the theoretically minimum value of 2.0, attributed to an infinite system. If k is indeed less than 2.0, it may reflect the finite size of the systems considered.

In this work it was essential to assume the formation of thermalized hot matter of nuclear dimensions; calculations of the time scale for such thermalization indicate that it may be possible during the expansion stage of the system and for temperatures greater than about 7—8 MeV.[33—35] It is fortunate that this time-constrained lower limit for the temperature of the system is substantially lower than that estimated by our analysis critical temperature of 11—12 MeV. Since a LG phase instability exists only for temperatures below the critical temperature and above the minimum temperature for phase equilibration, it is clear that if the latter temperature were higher than the former, the LG instability would not develop. We further rely on the freeze-out concept, which ensures that the experimentally observed mass distributions reflect satisfactorily the configuration of the expanding system at the freeze-out density. The close proximity of $\rho_f \sim \rho_c \sim 0.4\rho_0$ is encouraging. Both of the preceding concepts are generally accepted at high energies; there is, however, conflicting evidence whether equilibration is fully accomplished in the intermediate energy regime. Clearly, more experimental investigation with asymmetric systems is necessary to clarify this point.

This analysis demonstrates the interest and need to obtain systematic fragment distributions from proton-induced reactions, such as p + Ag, in the energy range between 1 and 20 GeV, as well as from heavy ion reactions, such as Ne + Ag, in the range of 30—70 MeV/nucleon, encompassing the region of the critical temperature. Such systematic studies and careful analysis should be able to distinguish any possible differences in the fragment production mechanism between proton- and heavy-ion-induced reactions, to accurately determine the critical quantities and eventually the equation of state for the hot nuclear system formed in such reactions. This information will be valuable in the study of other more exotic instabilities and forms of nuclear or hadron matter.

ACKNOWLEDGMENTS

We wish to thank the authors of Ref. 19 for making available their data before publication and D. H. Boal for interesting discussions. One of the authors (A.D.P.) wishes to thank the National Superconducting Cyclotron Laboratory (NSCL) at Michigan State University for hospitality extended while this work was carried out. This work was supported by NSF Grant No. PHY-83-12245.

[1]R. Stock *et al.*, Phys. Rev. Lett. **49**, 1236 (1982).
[2]A. D. Panagiotou *et al.*, Phys. Rev. Lett. **52**, 496 (1984).
[3]R. W. Minich *et al.*, Phys. Lett. **118B**, 458 (1982).
[4]P. J. Siemens, Nature (London) **305**, 410 (1983), and references therein.
[5]P. Danielewicz, Nucl. Phys. **A314**, 465 (1979).
[6]M. W. Curtin, H. Toki, and D. K. Scott, Phys. Lett. **123B**, 289 (1983).
[7]A. I. Warwick *et al.*, Phys. Rev. C **27**, 1083 (1983).
[8]G. Bertsch and P. J. Siemens, Phys. Lett. **126B**, 9 (1983).
[9]J. Cugnon, Phys. Lett. **135B**, 374 (1984).
[10]P. Bonche, S. Levit, and D. Vautherin, Service Physique Theorique Report 85, 1983.
[11]U. Mosel, P. G. Zint, and K. H. Passler, Nucl. Phys. **A236**, 252 (1974).
[12]B. Friedman and V. R. Pandharipande, Nucl. Phys. **A361**, 502 (1981).
[13]A. Z. Mekjian and D. S. Gupta, Phys. Rep. **C72**, 133 (1981).
[14]M.-C. Lemaire *et al.*, Phys. Lett. **85B**, 38 (1979).
[15]H. Schulz, D. N. Voskresensky, and J. Bondorf, Phys. Lett. **133B**, 141 (1983).
[16]J. E. Finn *et al.*, Phys. Rev. Lett. **49**, 1321 (1982).
[17]C. B. Chittwood *et al.*, Phys. Lett. **131B**, 289 (1983).
[18]R. E. L. Green and R. G. Korteling, Phys. Rev. C **22**, 1594 (1980).
[19]R. E. L. Green, R. G. Korteling, and K. P. Jackson, Phys. Rev. C **29**, 1806 (1984).
[20]G. D. Westfall *et al.*, Phys. Rev. C **17**, 1368 (1978).
[21]A. M. Poskanzer, G. W. Butler, and E. K. Hyde, Phys. Rev. C **3**, 882 (1971).
[22]U. Lynen *et al.*, Nucl. Phys. **A387**, 129c (1982).
[23]M. E. Fisher, Physics (N.Y.) **3**, 255 (1967).
[24]A. A. Caretto, J. Hudis, and G. Friedlander, Phys. Rev. **110**, 1130 (1958).
[25]A. S. Hirsch *et al.*, Phys. Rev. C **29**, 508 (1984).
[26]The cross section for the particle unstable ^{9}B is estimated to be about 15% of the total $Z=5$ cross section. An uncertainty of 10—15% in the relative cross section was used for all mass distribution.
[27]J. A. Gaigos *et al.*, Phys. Rev. Lett. **42**, 82 (1979).

[28]H. Jakaman, A. Z. Mekjian, and L. Zamick, Phys. Rev. C **27**, 1782 (1983).
[29]G. Sauer, H. Chandra, and U. Mosel, Nucl. Phys. **A264**, 221 (1976).
[30]W. Stocker and J. Burzlaff, Nucl. Phys. **A202**, 265 (1973).
[31]D. H. E. Gross *et al.*, Z. Phys. A **309**, 41 (1982).
[32]D. H. Boal, Michigan State University Cyclotron Laboratory Report MSUCL-451, 1984.
[33]D. H. Boal, Phys. Rev. C **28**, 2568 (1983).
[34]M. W. Curtin, H. Toki, and D. K. Scott, Michigan State University Cyclotron Laboratory Report MSUCL-426, 1983.
[35]D. K. Scott, Michigan State University Cyclotron Laboratory Report MSUCL-434, 1983.
[36]J. Bartel *et al.*, Theoretische Physik Universität Regensburg Report 21, 1983.
[37]The error bar for each point is the sum of the quoted uncertainties of the fragment yield for each fragment, added in quadrature.
[38]D. H. Boal, Michigan State University Cyclotron Laboratory Report MSUCL-458, 1984.
[39]D. J. Morrissey *et al.*, Michigan State University Cyclotron Laboratory Report MSUCL-454, 1984.